Elastic Wavefield Reconstruction Operators

Stuart Farris, Ettore Biondi, and Guillaume Barnier

ABSTRACT

We describe an Elastic Wavefield Reconstruction Inversion (EWRI) formulation and derive the necessary staggered grid wave equation operator. We then demonstrate that the elastic wave equation operator is the inverse of elastic wave propagation operator through a numerical example.

INTRODUCTION

There is a need for an earth parameter inversion technique that exceeds the ability of ray tracing, tomography, and dispersion analysis to estimate elastic earth properties by using all of the information contained in the recored data while simultaneously avoiding the computational complexity and nonlinearity of Full Waveform Inversion (FWI). A novel inversion scheme that alternately minimizes a data misfit term and a wave-equation misfit term was introduced by Van Leeuwen and Herrmann (2013), De Ridder and Maddison (2017), and De Ridder et al. (2017). The scheme first reconstructs an estimate of the wavefield that fits (in a least-squares sense) both a wave equation (given an estimate of the medium parameters) as well as recorded data. This wavefield is then used to update the earth model parameters with a wave equation inversion employing gradiometry to measure wavefield gradients (Curtis and Robertsson, 2002; Langston, 2007a,b; De Ridder and Biondi, 2015; De Ridder and Curtis, 2017). When the estimate of earth parameters is held constant, the reconstruction of the wavefield becomes a linear problem with respect to the wavefield. Likewise, when the wavefield is kept constant the problem becomes linear with respect to the earth model parameters. In this manner, the inversion scheme iteratively solves two linear inverse problems ultimately finding an optimal earth model and wavefield that match recorded data and some wave equation.

This technique is attractive because it does not require forward or adjoint wave propagation, is bilinear with respect to the wavefield and the earth parameters, and is linear with respect to seismic experiments, or shots. This frees the entire method from the stability issues associated with wave propagation, allowing much coarser discretization in time compared to other wave equation based velocity estimation techniques such as FWI. Furthermore, adding the minimization over the wavefield turns this into an extended wavefield inversion problem. In extended formulations, we expand the model space, beyond the physical earth parameters, to include some nonphysical space, in our case the wavefield. When our guess of the earth model is far from the truth, this nonphysical extension allows us to fit the data without projecting unfeasible updates to the physical model space. Then, as we iterate, we slowly eliminate the nonphysical part of the model and update the physical earth model, hopefully avoiding local minima.

Past Wavefield Reconstruction Inversion (WRI) work has assumed an acoustic earth and solved for p-wave velocity with frequency domain wave equation formulations where the discretized Helmholtz equation is factorized to obtain a direct inverse solution for wavefields. This factorization will become unfeasible due to computational cost when applied to three dimensional problems or problems with high levels of noise. Futhermore, complex wave modes, such as surface waves and converted waves, can not be modeled properly when assuming an acoustic earth.

Here we describe a time domain implementation of EWRI that accounts for an elastic, isotropic, attentuation-free earth. We also construct the operators necessary for the wavefield inversion step of EWRI.

ELASTIC WAVEFIELD RECONSTRUCTION INVERSION

The goal of EWRI is to estimate some material properties of the earth, $\mathbf{m}$, in some domain of the subsurface. Here we assume the subsurface is linear elastic and isotropic. We parameterize it with the Lame's first parameter, λ, shear modulus, μ, and density, ρ. Each point in the subsurface, $\mathbf{x}$, is associated with these three elastic parameters:

$$\mathbf{m}(\mathbf{x}) = \begin{bmatrix} \lambda \\ \mu \\ \rho \end{bmatrix}. \tag{1}$$

Following Virieux (1986) we can model how elastic energy interacts with the described subsurface with five wavefield components and five partial differential equations. The necessary wavefield components are particle velocity in the x direction, v_x, particle velocity in the z direction, v_z, and three components of the stress tensor, σ_{xx}, σ_{zz}, and σ_{xz}. We denote $\mathbf{p}$ as the vector describing the wavefield components for a given location in the subsurface $\mathbf{x}$, at a given time t, and for a given earth parameter function $\mathbf{m}$:

$$\mathbf{p}(\mathbf{x}, t; \mathbf{m}) = \begin{bmatrix} v_x \\ v_z \\ \sigma_{xx} \\ \sigma_{zz} \\ \sigma_{xz} \end{bmatrix}. \tag{2}$$

We use a wave equation operator, $\mathbf{A}$, which is a function of earth parameters, $\mathbf{m}$, to map from a wavefield, $\mathbf{p}(\mathbf{x}, t; \mathbf{m})$, to external forcing terms, $\mathbf{f}(\mathbf{x}, t)$:

$$\mathbf{A}(\mathbf{m})\mathbf{p} = \mathbf{f}. \tag{3}$$

Note how $\mathbf{p}$ and $\mathbf{f}$ are both functions of space $\mathbf{x}$ and time t. In our 2D space implementation, this means $\mathbf{p}$ and $\mathbf{f}$ live in the 3D space of x, z, and t. The full derivation of the wave equation operator, $\mathbf{A}(\mathbf{m})$, can be found in the Appendix. We know that the central difference first-order spatial derivatives in the elastic wave equation will produce significant numerical errors and therefore we must implement this operator on a staggered grid, seen in Figure 1 (Biondi and O'Reilly, 2015). We spatially stagger the elastic parameters, wavefield components, and derivative operators to construct our elastic wave equation operator.

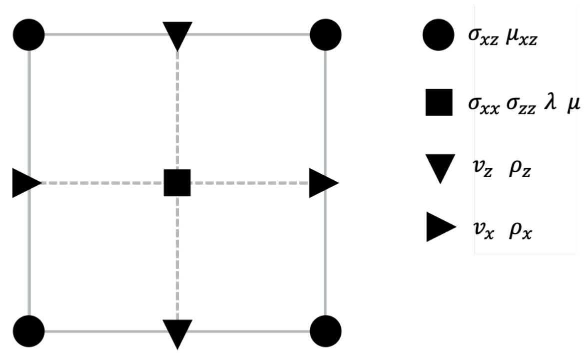

Figure 1: A representation of the different grids used to store the various wavefields needed for our elastic wave equation implementation. [**NR**]

With the elastic wave equation operator defined, we can introduce the EWRI objective function:

$$\Phi(\mathbf{m},\mathbf{p}) = \frac{1}{2}||\mathbf{K}\mathbf{p}-\mathbf{d}||_2^2 + \frac{\epsilon^2}{2}||\mathbf{A}(\mathbf{m})\mathbf{p}-\mathbf{f}||_2^2, \tag{4}$$

where $\mathbf{m}$, $\mathbf{p}$, $\mathbf{A}(\mathbf{m})$, and $\mathbf{f}$ have all been described previously. $\mathbf{d}$ is the observed data, recorded by physical receivers, and the sampling operator, $\mathbf{K}$, extracts the wavefield, $\mathbf{p}$, at those receiver locations. This objective function forces the reconstructed wavefield to match both the recorded data and to obey the wave equation in a least squares sense. As mentioned previously, this relaxes the physics of the problem by allowing the reconstructed wavefield to not fully obey the wave equation when the correct earth model parameters are not known.

Note that this objective function is bilinear. When either $\mathbf{m}$ or $\mathbf{p}$ are fixed, the objective function becomes linear with respect to the other variable. We minimize Equation 4 with respect to $\mathbf{m}$ or $\mathbf{p}$ with an alternating linear conjugate gradient scheme which is summarized in Algorithm 1. We first fix our earth model to an initial guess, $\mathbf{m}_0$, and minimize Equation 4 with respect to $\mathbf{p}$:

$$\Phi_{\mathbf{p}}(\mathbf{m}) = \frac{1}{2}||\mathbf{K}\mathbf{p}-\mathbf{d}||_2^2 + \frac{\epsilon^2}{2}||\mathbf{A}(\mathbf{m})\mathbf{p}-\mathbf{f}||_2^2 \tag{5}$$

Once some convergence criteria is met, we arrive at our first guess of the elastic wavefield, $\mathbf{p}$. Now we hold the wavefield constant and minimize Equation 4 with respect to $\mathbf{m}$:

$$\Phi_{\mathbf{m}}(\mathbf{p}) = \frac{1}{2}||\mathbf{K}\mathbf{p} - \mathbf{d}||_2^2 + \frac{\epsilon^2}{2}||\mathbf{A}(\mathbf{m})\mathbf{p} - \mathbf{f}||_2^2, \tag{6}$$

Since we reconstructed $\mathbf{p}$, in Equation 5, with an incorrect earth model, it will not be able to match both the recorded data and the elastic wave equation. This wave equation mismatch is used to update the earth model parameters when we minimize Equation 6.

Algorithm 1 Alternating Wavefield Reconstruction Inversion

```
given some observed wavefield, d
given a starting earth model, m_0
i = 0
while i < n do                                  ▷ for n iterations
    p_i ← arg min_p Φ_{m_i}(p) ← d, m_i         ▷ invert for optimal wavefield
    m_{i+1} ← arg min_m Φ_{p_i}(m) ← d, p_i     ▷ invert for new earth model
    i = i + 1
end while
return m_n                                      ▷ final earth model
```

WAVE EQUATION VS WAVE PROPAGATION

While elastic wave propagation is not necessary for the EWRI implementation, it is helpful to compare the elastic wave equation operator to the elastic wave propagator operator to put the two in context. As shown in Equation 3, the wave equation operator maps from a wavefield, $\mathbf{p}$, to a forcing term, $\mathbf{f}$. Conversely, elastic wave propagation maps from a forcing function, $\mathbf{f}$, to a wavefield, $\mathbf{p}$. In the Appendix we derive the staggered grid elastic wave propagation operator as $\mathbf{B}(\mathbf{m})$:

$$\mathbf{B}(\mathbf{m})\mathbf{f} = \mathbf{p}. \tag{7}$$

If we begin at some forcing term $\mathbf{f}$ and apply the wave propagation operator, $\mathbf{B}(\mathbf{m})$, we arrive at some wavefield, $\mathbf{p}$. If we substitute the resulting $\mathbf{p}$ into the wave equation operator, Equation 3, we will retrieve some other forcing term, $\mathbf{f}'$:

$$\mathbf{B}(\mathbf{m})\mathbf{f} = \mathbf{p}, \tag{8}$$
$$\mathbf{A}(\mathbf{m})\mathbf{B}(\mathbf{m})\mathbf{f} = \mathbf{f}'. \tag{9}$$

We can see that if $\mathbf{f} = \mathbf{f}'$ that $\mathbf{A}(\mathbf{m})\mathbf{B}(\mathbf{m}) = \mathbf{I}$ and therefore $\mathbf{A}(\mathbf{m}) = \mathbf{B}^{-1}(\mathbf{m})$. So if we propagate some wavefield from a seismic source, apply the wave equation operator to this wavefield, and the result is the original seismic source, we know that the wave equaton operator is the inverse of the wave propagation operator. This is important to rectify the physics of the wave equation operator. We can easily code some operator, it's correct adjoint, and verify this with the dot product test. Unfortunately, passing the dot product test gives no indication to whether or not the operator is applying the correct wave equation physics. If we cannot force the correct wave equation physics with our operator, there will be no hope of EWRI converging to correct solutions.

INVERSE PROPERTY NUMERICAL EXAMPLE

Here we show a simple example to verify that $\mathbf{A}(\mathbf{m}) = \mathbf{B}^{-1}(\mathbf{m})$. We assume the elastic earth model, $\mathbf{m}$, is known and is a half space, seen in Figure 2. A symmetric explosive source, $\mathbf{f}$, with frequencies ranging from 4-16 Hz is injected in the top left corner of the model also illustrated in Figure 2. We show the five components of $\mathbf{f}$ at $\mathbf{f}(\mathbf{x} = \mathbf{x}_s, t)$, where $\mathbf{x}_s$ is the location in space where the source was injected, in Figure 3. Since $\mathbf{f}$ is a volumetric source, the only nonzero components are σ_{xx} and σ_{zz}. Applying the recursive wave propagation operator to results in $\mathbf{p} = \mathbf{B}(\mathbf{m})\mathbf{f}$. A snapshot at $t = 1.75$ sec of each component of the wavefield, $\mathbf{p}$, is illustrated in Figure 4. We see that a volumetric source results in all wavefield components being excited during propagation. We can now apply the wave equation operator, $\mathbf{A}(\mathbf{m})$, to the propagated wavefield, $\mathbf{p}$, which results in another forcing term, $\mathbf{f'}$, plotted at $\mathbf{x} = \mathbf{x}_s$ in Figure 5. Visually, it appears we have recovered the original forcing term, as $\mathbf{f}'$ seems identical to $\mathbf{f}$. However, when we take the difference between the two, we notice that there is about a 2 percent discrepancy in the σ_{xx} and σ_{zz} components, which is illustrated in Figure 6.

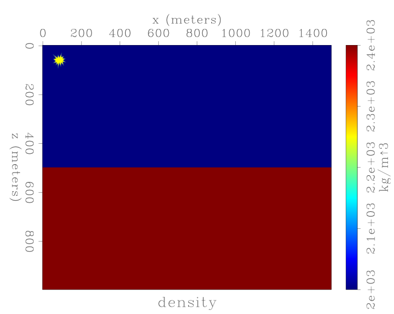

Figure 2: Known elastic earth model, $\mathbf{m}$, used to verify that $\mathbf{A}(\mathbf{m}) = \mathbf{B}^{-1}(\mathbf{m})$. Displayed is the elastic parameter density, ρ. The other two parameters, λ and μ, are also half spaces but are not displayed for sake of redundancy. Source injection point is labeled with the yellow marker in the top left corner. [**ER**]

CONCLUSION

We have introduced the elastic formulation of WRI. In order to match converted wave modes and surface wave scattering we must use an elastic wave equation operator

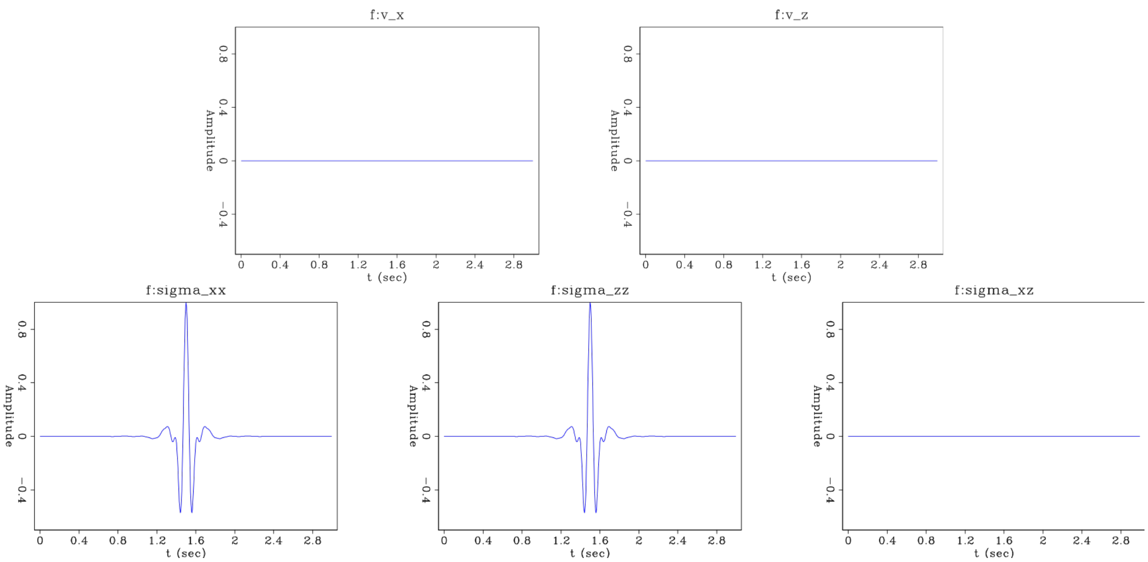

Figure 3: The five components of the forcing term $\mathbf{f}$ [**ER**]

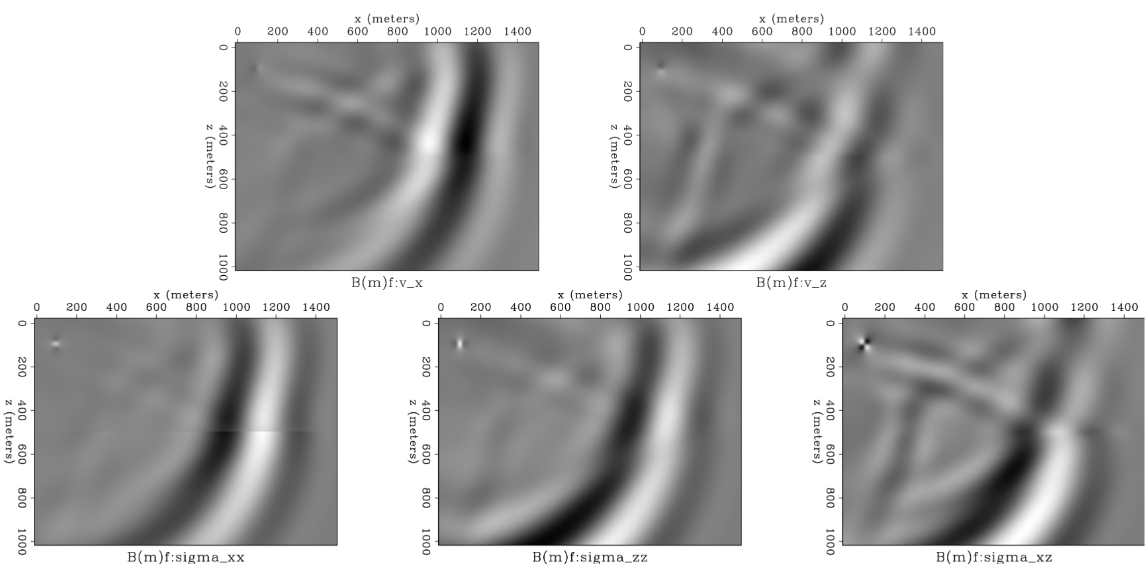

Figure 4: A snapshot at $t = 1.75$ sec of the wavefield components of $\mathbf{p}$, the result of applying the wave propagation operator to the forcing term. $\mathbf{p} = \mathbf{B}(\mathbf{m})\mathbf{f}$ [**ER**]

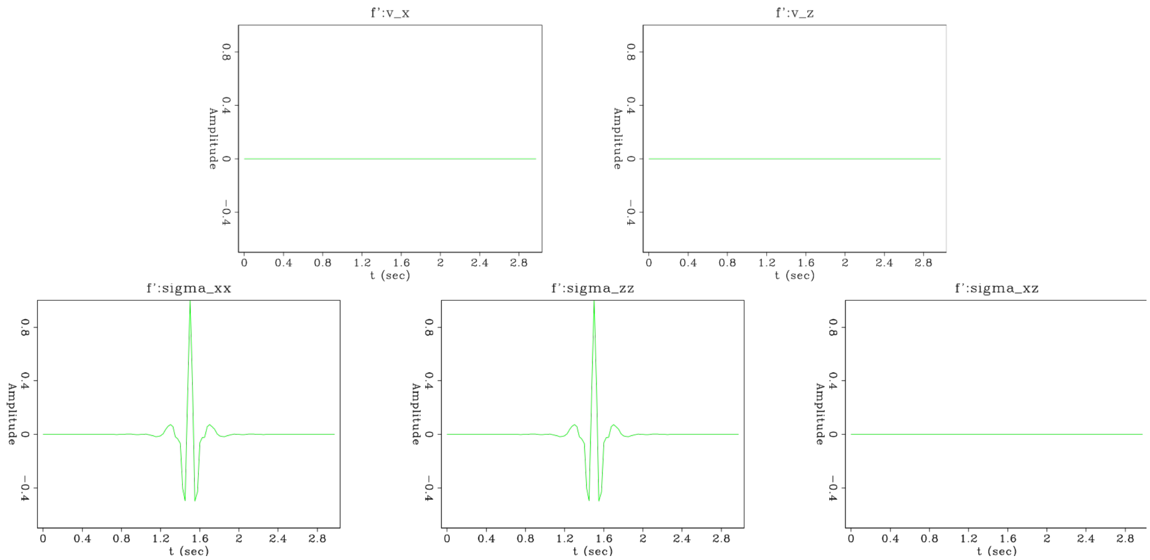

Figure 5: The five components of the recovered forcing term $\mathbf{f'} = \mathbf{A}(\mathbf{m})\mathbf{B}(\mathbf{m})\mathbf{f}$ [**ER**]

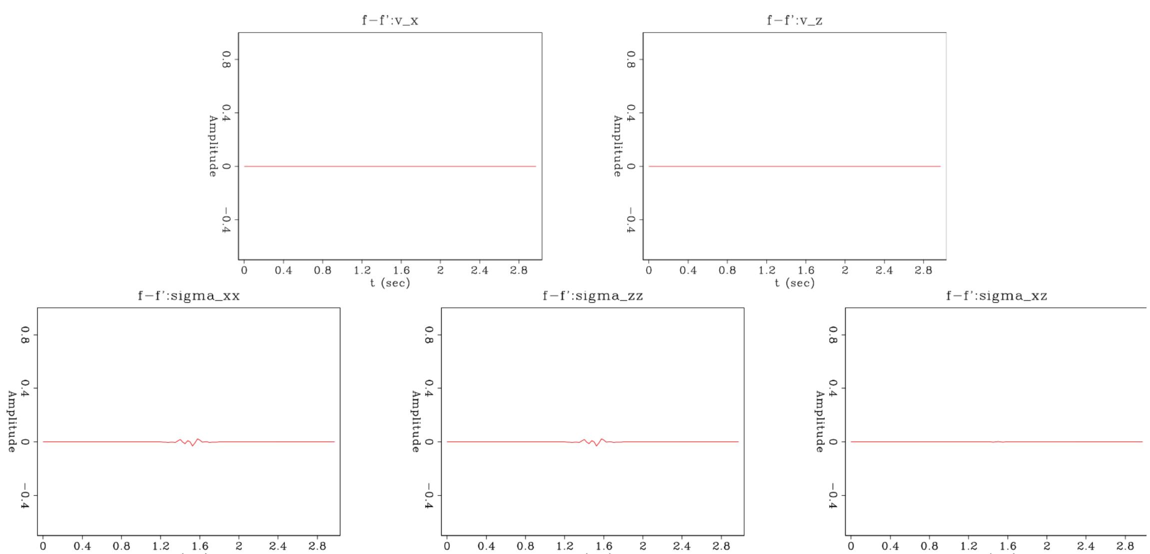

Figure 6: The difference between the original forcing term and the recovered forcing term, $\mathbf{f} - \mathbf{f}'$. Notice the 2 percent error in the σ_{xx} and σ_{zz} components. We believe this error arises from the limited bandwidth of the spatial derivative stencil in the wave equation operator. [**ER**]

which we derive in the Appendix. We show that the elastic wave equation operator is applying the same physics as the elastic wave propagation operator through a numerical example.

ACKNOWLEDGEMENT

First and foremost, Guillaume Barnier should be thanked for his extremely fast, well commented, and thorough 2D acoustic GPU wave equation propagation code that was used as a template for our own elastic wave equation and propagation code. Thank you to the SEP affiliates for their continued mentorship and financial support.

APPENDIX

Deriving the staggered grid elastic wave equation operator

The wave equations to describe relationship of the five elastic wavefield components are:

$$\begin{aligned}
\rho\frac{\partial v_x}{\partial t} - \frac{\partial \sigma_{xx}}{\partial x} - \frac{\partial \sigma_{xz}}{\partial z} &= f_x, \\
\rho\frac{\partial v_z}{\partial t} - \frac{\partial \sigma_{xz}}{\partial x} - \frac{\partial \sigma_{zz}}{\partial z} &= f_z, \\
\frac{\partial \sigma_{xx}}{\partial t} - (\lambda + 2\mu)\frac{\partial v_x}{\partial x} - \lambda\frac{\partial v_z}{\partial z} &= S_{xx}, \\
\frac{\partial \sigma_{zz}}{\partial t} - \lambda\frac{\partial v_x}{\partial x} - (\lambda + 2\mu)\frac{\partial v_z}{\partial z} &= S_{zz}, \\
\frac{\partial \sigma_{xz}}{\partial t} - \mu\left(\frac{\partial v_x}{\partial z} + \frac{\partial v_z}{\partial x}\right) &= S_{xz},
\end{aligned} \tag{10}$$

where f_x, f_z, S_{xx}, S_{xz}, and S_{xz} are the external forcing terms (aka seismic sources for each component). We assume that $\mathbf{p}(\mathbf{x}, t = 0; \mathbf{m}) = \mathbf{0}$ and an absorbing boundary condition Engquist (1976). It is convenient to write this as a matrix, vector multiplication:

$$\begin{bmatrix}
\rho\frac{\partial}{\partial t} & 0 & -\frac{\partial}{\partial x} & 0 & -\frac{\partial}{\partial z} \\
0 & \rho\frac{\partial}{\partial t} & 0 & -\frac{\partial}{\partial z} & -\frac{\partial}{\partial x} \\
-(\lambda + 2\mu)\frac{\partial}{\partial x} & -\lambda\frac{\partial}{\partial z} & \frac{\partial}{\partial t} & 0 & 0 \\
-\lambda\frac{\partial}{\partial x} & -(\lambda + 2\mu)\frac{\partial}{\partial z} & 0 & \frac{\partial}{\partial t} & 0 \\
-\mu\frac{\partial}{\partial z} & -\mu\frac{\partial}{\partial x} & 0 & 0 & \frac{\partial}{\partial t}
\end{bmatrix}
\begin{bmatrix} v_x \\ v_z \\ \sigma_{xx} \\ \sigma_{zz} \\ \sigma_{xz} \end{bmatrix}
=
\begin{bmatrix} f_x \\ f_z \\ S_{xx} \\ S_{zz} \\ S_{xz} \end{bmatrix}. \tag{11}$$

We rewrite the derivatives with operator notation for further convenience:

$$\begin{bmatrix}
\rho\mathbf{D}_t & 0 & -\mathbf{D}_x & 0 & -\mathbf{D}_z \\
0 & \rho\mathbf{D}_t & 0 & -\mathbf{D}_z & -\mathbf{D}_x \\
-(\lambda + 2\mu)\mathbf{D}_x & -\lambda\mathbf{D}_z & \mathbf{D}_t & 0 & 0 \\
-\lambda\mathbf{D}_x & -(\lambda + 2\mu)\mathbf{D}_z & 0 & \mathbf{D}_t & 0 \\
-\mu\mathbf{D}_z & -\mu\mathbf{D}_x & 0 & 0 & \mathbf{D}_t
\end{bmatrix}
\begin{bmatrix} v_x \\ v_z \\ \sigma_{xx} \\ \sigma_{zz} \\ \sigma_{xz} \end{bmatrix}
=
\begin{bmatrix} f_x \\ f_z \\ S_{xx} \\ S_{zz} \\ S_{xz} \end{bmatrix}. \tag{12}$$

We know that the central difference first-order spatial derivatives, $\mathbf{D}_x$ and $\mathbf{D}_z$, will produce significant numerical errors (Biondi and O'Reilly, 2015). Therefore we must implement these operators on a staggered grid, seen in Figure 1. We center the derivatives appropriately and rewrite the wave equation matrix as:

$$\begin{bmatrix} \rho_x \mathbf{D}_t & 0 & -\mathbf{D}_x^- & 0 & -\mathbf{D}_z^+ \\ 0 & \rho_z \mathbf{D}_t & 0 & -\mathbf{D}_z^- & -\mathbf{D}_x^+ \\ -(\lambda+2\mu)\mathbf{D}_x^+ & -\lambda \mathbf{D}_z^+ & \mathbf{D}_t & 0 & 0 \\ -\lambda \mathbf{D}_x^+ & -(\lambda+2\mu)\mathbf{D}_z^+ & 0 & \mathbf{D}_t & 0 \\ -\mu_{xz}\mathbf{D}_z^- & -\mu_{xz}\mathbf{D}_x^- & 0 & 0 & \mathbf{D}_t \end{bmatrix} \begin{bmatrix} v_x \\ v_z \\ \sigma_{xx} \\ \sigma_{zz} \\ \sigma_{xz} \end{bmatrix} = \begin{bmatrix} f_x \\ f_z \\ S_{xx} \\ S_{zz} \\ S_{xz} \end{bmatrix}, \tag{13}$$

where $\mathbf{D}^+$ and $\mathbf{D}^-$ are the forward and backward derivative operators, respectively. Now the staggered elastic parameters, wavefield components, and derivative operators, force each line of the wave equation matrix operation to fall on the same spatial grid location, thus eliminating the unwanted numerical errors. Equation 13 describes our elastic wave equation and we denote $\mathbf{A}(\mathbf{m})$ as the matrix acting on the wavefield components of $\mathbf{p}$:

$$\mathbf{A}(\mathbf{m})\mathbf{p} = \mathbf{f} \tag{14}$$

Deriving the staggered grid elastic wave propagation operator

We can derive a recursive time-stepping scheme to map from our forcing term $\mathbf{f}$ resulting in a wavefield $\mathbf{p}$. We begin from the wave equation operator in Equation 13 and isolate each equation from the matrix, vector multiplication:

$$\begin{aligned} \rho_x \mathbf{D}_t v_x - \mathbf{D}_x^- \sigma_{xx} - \mathbf{D}_z^+ \sigma_{xz} &= f_x \\ \rho_z \mathbf{D}_t v_x - \mathbf{D}_z^- \sigma_{zz} - \mathbf{D}_x^- \sigma_{xz} &= f_z \\ \mathbf{D}_t \sigma_{xx} - (\lambda+2\mu)\mathbf{D}_x^+ v_x - \lambda \mathbf{D}_z^+ v_z &= S_{xx} \\ \mathbf{D}_t \sigma_{zz} - \lambda \mathbf{D}_x^+ v_x - (\lambda+2\mu)\mathbf{D}_z^+ v_z &= S_{zz} \\ \mathbf{D}_t \sigma_{xz} - \mu_{xz}\mathbf{D}_z^- v_x - \mu_{xz}\mathbf{D}_x^- v_z &= S_{xz} \end{aligned} \tag{15}$$

For each equation, isolate the time derivative operation.

$$\begin{aligned} \rho_x \mathbf{D}_t v_x &= \mathbf{D}_x^- \sigma_{xx} + \mathbf{D}_z^+ \sigma_{xz} + f_x \\ \rho_z \mathbf{D}_t v_x &= \mathbf{D}_z^- \sigma_{zz} + \mathbf{D}_x^- \sigma_{xz} + f_z \\ \mathbf{D}_t \sigma_{xx} &= (\lambda+2\mu)\mathbf{D}_x^+ v_x + \lambda \mathbf{D}_z^+ v_z + S_{xx} \\ \mathbf{D}_t \sigma_{zz} &= \lambda \mathbf{D}_x^+ v_x + (\lambda+2\mu)\mathbf{D}_z^+ v_z + S_{zz} \\ \mathbf{D}_t \sigma_{xz} &= \mu_{xz}\mathbf{D}_z^- v_x + \mu_{xz}\mathbf{D}_x^- v_z + S_{xz} \end{aligned} \tag{16}$$

By using a centered finite difference stencil for the time derivatives, we can rewrite the equation with the proper time steps on each component:

$$
\begin{aligned}
\rho_x \frac{v_x(t_{i+\frac{1}{2}}) - v_x(t_{i-\frac{1}{2}})}{\Delta t} &= \mathbf{D}_x^- \sigma_{xx}(t_i) + \mathbf{D}_z^+ \sigma_{xz}(t_i) + f_x(t_i) \\
\rho_z \frac{v_z(t_{i+\frac{1}{2}}) - v_z(t_{i-\frac{1}{2}})}{\Delta t} &= \mathbf{D}_z^- \sigma_{zz}(t_i) + \mathbf{D}_x^- \sigma_{xz}(t_i) + f_z(t_i) \\
\frac{\sigma_{xx}(t_{i+\frac{1}{2}}) - \sigma_{xx}(t_{i-\frac{1}{2}})}{\Delta t} &= (\lambda + 2\mu)\mathbf{D}_x^+ v_x(t_i) + \lambda \mathbf{D}_z^+ v_z(t_i) + S_{xx}(t_i) \\
\frac{\sigma_{zz}(t_{i+\frac{1}{2}}) - \sigma_{zz}(t_{i-\frac{1}{2}})}{\Delta t} &= \lambda \mathbf{D}_x^+ v_x(t_i) + (\lambda + 2\mu)\mathbf{D}_z^+ v_z(t_i) + S_{zz}(t_i) \\
\frac{\sigma_{xz}(t_{i+\frac{1}{2}}) - \sigma_{xz}(t_{i-\frac{1}{2}})}{\Delta t} &= \mu_{xz} \mathbf{D}_z^- v_x(t_i) + \mu_{xz} \mathbf{D}_x^- v_z(t_i) + S_{xz}(t_i)
\end{aligned}
$$

Notice the time derivatives are centered at $t = t_i$ and are computed using wavefields at $t = t_{i+\frac{1}{2}}$ and $t = t_{i-\frac{1}{2}}$. Using half-time step discretization is an implementation decision made to increase the accuracy of the time derivatives (as compared to using $t = t_{i+1}$ and $t = t_{i-1}$). To arrive at a recursive time-stepping scheme, we solve each equation for the wavefield at $t = t_{i+\frac{1}{2}}$.

$$
v_x(t_{i+\frac{1}{2}}) = v_x(t_{i-\frac{1}{2}}) + \frac{\Delta t}{\rho_x} \left[\mathbf{D}_x^- \sigma_{xx}(t_i) + \mathbf{D}_z^+ \sigma_{xz}(t_i) + f_x(t_i) \right] \tag{17}
$$

$$
v_z(t_{i+\frac{1}{2}}) = v_z(t_{i-\frac{1}{2}}) + \frac{\Delta t}{\rho_x} \left[\mathbf{D}_z^- \sigma_{zz}(t_i) + \mathbf{D}_x^- \sigma_{xz}(t_i) + f_z(t_i) \right] \tag{18}
$$

$$
\sigma_{xx}(t_{i+\frac{1}{2}}) = \sigma_{xx}(t_{i-\frac{1}{2}}) + \Delta t \left[(\lambda + 2\mu)\mathbf{D}_x^+ v_x(t_i) + \lambda \mathbf{D}_z^+ v_z(t_i) + S_{xx}(t_i) \right] \tag{19}
$$

$$
\sigma_{zz}(t_{i+\frac{1}{2}}) = \sigma_{zz}(t_{i-\frac{1}{2}}) + \Delta t \left[\lambda \mathbf{D}_x^+ v_x(t_i) + (\lambda + 2\mu)\mathbf{D}_z^+ v_z(t_i) + S_{zz}(t_i) \right] \tag{20}
$$

$$
\sigma_{xz}(t_{i+\frac{1}{2}}) = \sigma_{xz}(t_{i-\frac{1}{2}}) + \Delta t \left[\mu_{xz} \mathbf{D}_z^- v_x(t_i) + \mu_{xz} \mathbf{D}_x^- v_z(t_i) + S_{xz}(t_i) \right] \tag{21}
$$

We can shift the time sample by one half to simplify the the operator into a lower traingular matrix:

$$
v_x(t_i) = v_x(t_{i-1}) + \frac{\Delta t}{\rho_x} \left[\mathbf{D}_x^- \sigma_{xx}(t_{i-\frac{1}{2}}) + \mathbf{D}_z^+ \sigma_{xz}(t_{i-\frac{1}{2}}) + f_x(t_{i-\frac{1}{2}}) \right], \tag{22}
$$

$$
v_z(t_i) = v_z(t_{i-1}) + \frac{\Delta t}{\rho_x} \left[\mathbf{D}_z^- \sigma_{zz}(t_{i-\frac{1}{2}}) + \mathbf{D}_x^- \sigma_{xz}(t_{i-\frac{1}{2}}) + f_z(t_{i-\frac{1}{2}}) \right], \tag{23}
$$

$$
\sigma_{xx}(t_i) = \sigma_{xx}(t_{i-1}) + \Delta t \left[(\lambda + 2\mu)\mathbf{D}_x^+ v_x(t_{i-\frac{1}{2}}) + \lambda \mathbf{D}_z^+ v_z(t_{i-\frac{1}{2}}) + S_{xx}(t_{i-\frac{1}{2}}) \right], \tag{24}
$$

$$
\sigma_{zz}(t_i) = \sigma_{zz}(t_{i-1}) + \Delta t \left[\lambda \mathbf{D}_x^+ v_x(t_{i-\frac{1}{2}}) + (\lambda + 2\mu)\mathbf{D}_z^+ v_z(t_{i-\frac{1}{2}}) + S_{zz}(t_{i-\frac{1}{2}}) \right], \tag{25}
$$

$$
\sigma_{xz}(t_i) = \sigma_{xz}(t_{i-1}) + \Delta t \left[\mu_{xz} \mathbf{D}_z^- v_x(t_{i-\frac{1}{2}}) + \mu_{xz} \mathbf{D}_x^- v_z(t_{i-\frac{1}{2}}) + S_{xz}(t_{i-\frac{1}{2}}) \right]. \tag{26}
$$

We denote $\mathbf{B}(\mathbf{m})$ as the recursive operator acting on the forcing term $\mathbf{f}$ resulting in a wavefield $\mathbf{p}$:

$$
\mathbf{B}(\mathbf{m})\mathbf{f} = \mathbf{p}. \tag{27}
$$

REFERENCES

Biondi, E., and O. O'Reilly, 2015, Two-way wave-equation operators for non-constant density acoustic isotropic media.

Curtis, A., and J. O. A. Robertsson, 2002, Volumetric wavefield recording and wave equation inversion for near-surface material properties: Geophysics, **67**, 1602–1611.

De Ridder, S., and B. L. Biondi, 2015, Near-surface Scholte wave velocities at Ekofisk from short noise recordings by seismic noise gradiometry: Geophysical Research Letters, **42**, 7031–7038.

De Ridder, S., and A. Curtis, 2017, Seismic Gradiometry using Ambient Seismic Noise in an Anisotropic Earth: Geophysical Journal International, **209**, 1168–1179.

De Ridder, S., A. Curtis, J. r. Maddison, and A. Shaiban, 2017, Frequency-domain full-wavefield inversion for ambient seismic surface-wave noise, *in* SEG Technical Program Expanded Abstracts 2017: Society of Exploration Geophysicists, 2877–2882.

De Ridder, S., and J. R. Maddison, 2017, Wave field inversion of ambient seismic noise: Presented at the 79$ˆ{th}$ Conference and Exhibition, EAGE, Extended Abstracts.

Engquist, B., 1976, Absorbing boundary conditions for wave equations.

Langston, C. A., 2007a, Spatial Gradient Analysis for Linear Seismic Arrays: Bulletin of the Seismological Society of America, **97**, 265–280.

———, 2007b, Wave Gradiometry in Two Dimensions: Bulletin of the Seismological Society of America, **97**, 401–416.

Van Leeuwen, T., and F. J. Herrmann, 2013, Mitigating local minima in full-waveform inversion by expanding the search space: Geophysical Journal International, **195**, 661–667.

Virieux, J., 1986, P-SV wave propagation in heterogeneous media: Velocity-stress finite-difference method: Geophysics, **51**.